ELSEVIER

Journal of Nuclear Materials 266–269 (1999) 365–369

journal of nuclear materials

Spectroscopic investigation of the dynamics of ions and neutrals in the ASDEX Upgrade Divertor II

J. Gafert [a,b,*], K. Behringer [b], D. Coster [b], C. Dorn [b], A. Kallenbach [b], R. Schneider [b], U. Schumacher [a], ASDEX Upgrade Team [b]

[a] *Institut für Plasmaforschung, Universität Stuttgart, Pfaffenwaldring 31, D-70556 Stuttgart, Germany*
[b] *MPI für Plasmaphysik, E4, EURATOM Association, Boltzmannstr. 2, D-85748 Garching, Germany*

Abstract

Detachment at the separatrix is a promising possibility to reduce the peak power load onto the divertor target plates. We investigated this topic spectroscopically at ASDEX Upgrade by measuring particle velocities using Doppler spectroscopy. The experimental data show a reduction of the chord averaged hydrogen velocity along the separatrix by about a factor of 3. Another important subject is flow reversal: after a brief discussion of 2D-code predictions and the conditions for detection we present spectroscopic evidence for flow reversal of C^{2+}-ions in the ASDEX Upgrade divertor II. The comparison of these spectroscopic data with B2-EIRENE modeling shows good qualitative and quantitative agreement.

Keywords: ASDEX Upgrade; Hydrogen; B2/EIRENE; Carbon impurities; Detachment; Divertor spectroscopy; Flow reversal; Particle flow; Recombination

1. Introduction

For an optimized design of the divertor and its operation in future fusion reactors it is essential to study divertor physics in present day fusion experiments. One of the most challenging problems is the reduction of the target power load to values acceptable from an engineering point of view and compatible with the requirement of particle exhaust and core confinement. A promising possibility to achieve this goal is a complete detachment defined by a drop of the ion saturation current by at least one order of magnitude due to a significant increase of volume recombination: the ion flux is stopped in the volume in front of the target plates, and accordingly, the energy deposited in the plates by surface recombination processes (13.6 eV per ion for hydrogen) is strongly reduced.

However, even for detached divertor conditions the property of the divertor to retain impurities from the main plasma has to be maintained. One effect predicted by theory and modeling and acting against the retention capability is the local backflow of impurities towards the main plasma – commonly denoted as 'flow reversal' [1].

In this paper, we discuss detachment and flow reversal, two topics that have recently been investigated spectroscopically at ASDEX Upgrade. High-resolution Doppler spectroscopy is a technique that was demonstrated to be suitable for obtaining flow velocities of ions and atoms [2]. For the ASDEX Upgrade divertor II configuration the spatial resolution is achieved by a fiberoptic system consisting of an overall number of 150 lines of sight. With two sets of chords aligned perpendicular to the magnetic field lines in a poloidal plane (Fig. 1 (a)), the strikepoint region of each divertor (inner and outer) is observed. Making use of these chords, detachment is well monitored by the temporal evolution of the spatial CIII-emission profiles in front of the plates. Two other groups are oriented roughly toroidally, one mainly parallel to the magnetic field direction and the other one anti-parallel to it. They allow, owing to the opposite signs of their Doppler shifts, a reliable determination of flow velocities in the divertor. This

* Corresponding author. Tel.: +49-89 3299 2214; fax: +49-89 3299 1812; e-mail: gafert@ipp.mpg.de.

0022-3115/99/$ – see front matter
PII: S0022-3115(98)00668-0

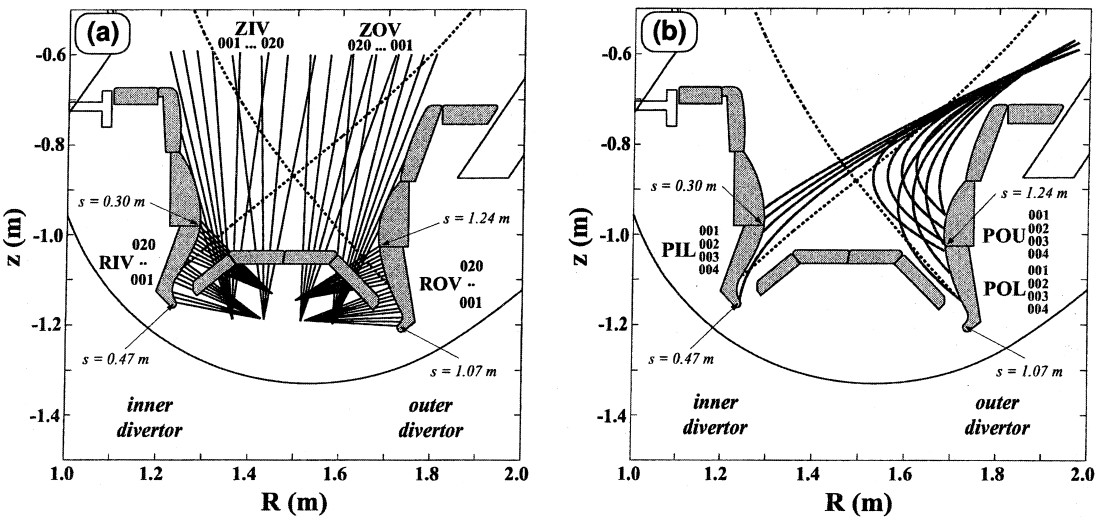

Fig. 1. (a) Poloidal lines of sight in the ASDEX Upgrade Divertor II. The area in front of the target plates can be probed with high-spatial resolution. The X-point region is covered by chords viewing in z-direction. The definition of the s-coordinate in the divertor is indicated. (b) Twelve (out of a total of 40) toroidal lines of sight in the ASDEX Upgrade Divertor II projected into a poloidal plane. The outer and inner divertor area are covered to allow for spatially resolved velocity measurements.

line-of-sight arrangement was chosen on the basis of B2-EIRENE [3] predictive calculations and optimized with respect to the possibility of observing flow reversal [4]. The projections of these chords into a poloidal plane are shown in Fig. 1(b) and demonstrate that particle flows can be measured unambiguously in the outer divertor and in many cases in the inner divertor as well. A complete quartz fiber coupling system permits the combination of all these lines of sight with spectrometers of different resolution and consequently, increases the flexibility significantly.

2. Experimental results on hydrogen dynamics during detachment

In order to explore the dependence of particle velocities on the detachment process, a density ramp was performed. Due to the high H-mode threshold with hydrogen as a working gas it was possible to keep the discharge in L-mode. During this density ramp, achieved by gas puffing combined with a stepwise increase of hydrogen neutral beam injection, the divertor conditions alternated between attached and detached. Fig. 2(a) shows the neutral beam injected power and the midplane and divertor densities as a function of time. The CIII-emission in front of the outer target plates (strikepoint region) is plotted in Fig. 2(b) and serves as a monitor for detachment. At the same time as the CIII-emission moves upstream the H_β-emission (Fig. 2(c), solid line) measured along toroidal chord POL004 (along the separatrix; comp. Fig. 1(b)) rises. While for low density this increase is rather weak, it is considerably larger at high densities ($t > 2.9$ s). The latter case reflects the strong volume recombination discussed above as the reason for detachment. The strongly inclined target plates of ASDEX Upgrade divertor II reflect the neutrals preferentially towards the separatrix. This leads to high densities in this region and has two important consequences [5]:

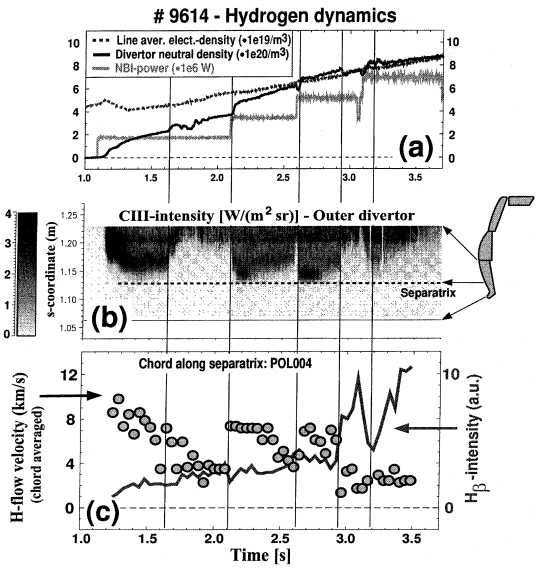

Fig. 2. Hydrogen dynamics at the separatrix in an L-mode density ramp: (a) line averaged electron density, divertor neutral density and NBI-power; (b) CIII-emission in the strikepoint region as detachment monitor; (c) evolution of hydrogen intensity and (chord averaged) velocity in the density ramp: during detachment the H-velocity is strongly reduced.

first, detachment starts rather early close to the separatrix and then extends further into the scrape-off layer (SOL). Second, neutrals and ions are strongly coupled through charge exchange, and accordingly, are in thermal equilibrium under these conditions. Therefore, during detachment, it is straightforward to consider the hydrogen *neutral* flow velocities determined from the Doppler shift of the highly resolved H_β-emission spectra as velocities of the hydrogen *ions*. Under attached conditions, the deduction of the fuel ion velocity from the Doppler shift of the neutrals is more problematical, because the velocity distribution of the ions may be affected by Frank–Condon neutrals, by an asymmetry in the velocity created by particles recycling at the target plates or by bi-Maxwellian distributions. Hence, for lower density conditions where ions and neutrals are no longer in thermal equilibrium, the ion velocity is not to be obtained reliably from this kind of measurement. However, due to the geometry effect discussed above, the situation in the ASDEX Upgrade divertor II is quite different from other tokamaks: the vertical inclination of the target plates leads, by the directed reflection of neutrals towards the separatrix, to rather high densities already under attached conditions. We stress that these 'attached' conditions (in ASDEX Upgrade divertor II) are already close to conditions that are called 'partially detached' in other tokamaks (with an open divertor). Therefore, thermal equilibrium is also expected to be good enough for the attached conditions considered here and the velocity of the neutrals can, despite the possible complications discussed above, be regarded as that of the fuel ions.

A comparison of the time dependence of the hydrogen velocity along the separatrix (Fig. 2(c), solid circles) with the CIII- and H_β-emission clearly demonstrates the reduction of the – chord averaged – velocity by about a factor of 3 during detachment. If radiation losses of hydrogen or carbon are large enough that divertor temperatures decrease below about 1.5 eV (detached conditions) there is an onset of strong net recombination if the ions flowing towards the target have enough time to recombine. In order to sustain this net recombination the ion flow velocities have to be strongly reduced. This is obtained by enhanced momentum losses by charge exchange with neutrals. Hence, the ion flux onto the divertor plates is drastically reduced due to the recombination in the plasma volume in front of the target.

B2-EIRENE results were selected for the appropriate densities and input powers for the attached and detached phases in this discharge and averaged over chord POL004. This yields values of 8–12 and 2–3 km/s, respectively. The corresponding experimental velocities from Fig. 2(c) are 7–9 km/s (well attached) and 1.5–3.5 km/s (well detached). For the two B2-EIRENE cases used the velocity difference between ions and neutrals along the toroidal chord POL004 is not more than about 20%, supporting our interpretation of the measured velocities of the hydrogen neutrals as ion flows. Therefore, two statements can be made: first, the absolute values of modeling and experiment agree well. Second, the predicted velocity reduction during detachment is also clearly confirmed by the spectroscopic measurement presented in Fig. 2.

3. Observation of C^{2+}-flow reversal during detachment

In the course of detachment – with increasing divertor density – the temperature gradient from the target plates to the X-point region also increases. Therefore, the resulting thermal forces directed away from the target that drive flow reversal of impurities become more important than the 'normal' forces (electric, pressure, friction) towards the target. If the local Mach number of the fuel ions becomes smaller than the ratio of the (impurity) ion mean free path to the (fuel ion) temperature gradient length flow reversal can appear [1]. Hence, for a limited density range, where the plasma is sufficiently detached for a strong temperature gradient to exist, the flow of impurity ions is expected to be reversed. A closer approach to the density limit which is related to complete detachment and to the appearance of a MARFE on closed fieldlines might again switch off flow reversal: the cooling of the SOL by radiation losses on closed field lines can reduce the SOL temperature gradients so strongly that the thermal force is no longer able to overcome the forward driving forces.

To be able to detect flow reversal spectroscopically the spatial overlap of the respective emission and flow reversal regions has to be large enough. It is not possible to quantify this in general, because it depends on the kind of spectral line shape, ion temperature and on the velocities themselves, which amount of overlap is required to determine a reversed flow from the measured spectrum reliably. For the CIII-triplet line ($\lambda = 465$ nm) the intensity contribution of the reversed flow component in the spectrum should be at least 25%. B2-EIRENE simulations for different densities predict that the CIII-emission in the respective flow reversal zone should be sufficient to be measured under the slightly detached conditions described above. From Fig. 3 it is obvious that this required overlap is only given for chord POU004. Accordingly, the resulting CIII-spectrum in this toroidal line of sight should be composed of a 'normally' (e.g. blue) Doppler shifted component and an oppositely shifted (e.g. red) one, due to the ions flowing back.

Fig. 4(a) and (b) show the CIII-spectra (toroidal chord POU004) obtained in an L-mode density ramp (# 9761) for attached (*a*, $t = 2.8$ s) and detached (*b*, $t = 3.2$ s) conditions, respectively. While the first spectrum (Fig. 4(a)) is blue-shifted (relative to the dashed line

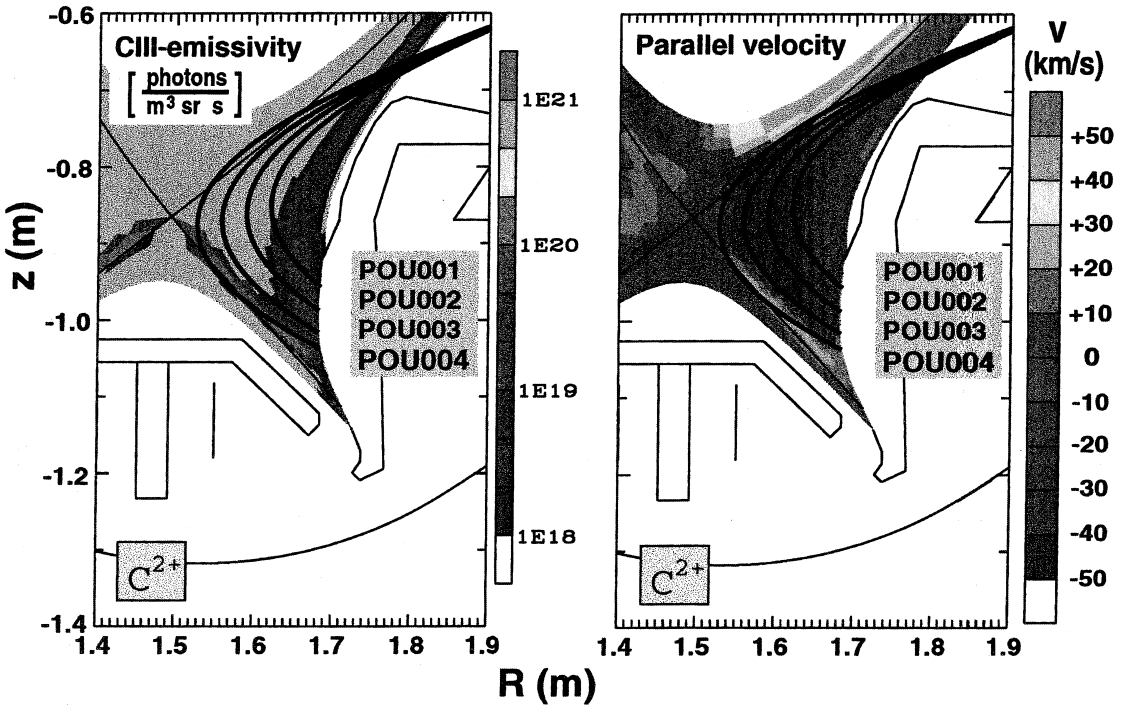

Fig. 3. B2-EIRENE modeling of C^{2+}-emissivity and C^{2+}-velocity (parallel to the magentic field lines); as the required overlap of the CIII-emission with the flow reversal zones (blue areas in the right figure) is limited to small regions in front of the target plates and near the X-point flow reversal is spectroscopically detectable only in chord POU004.

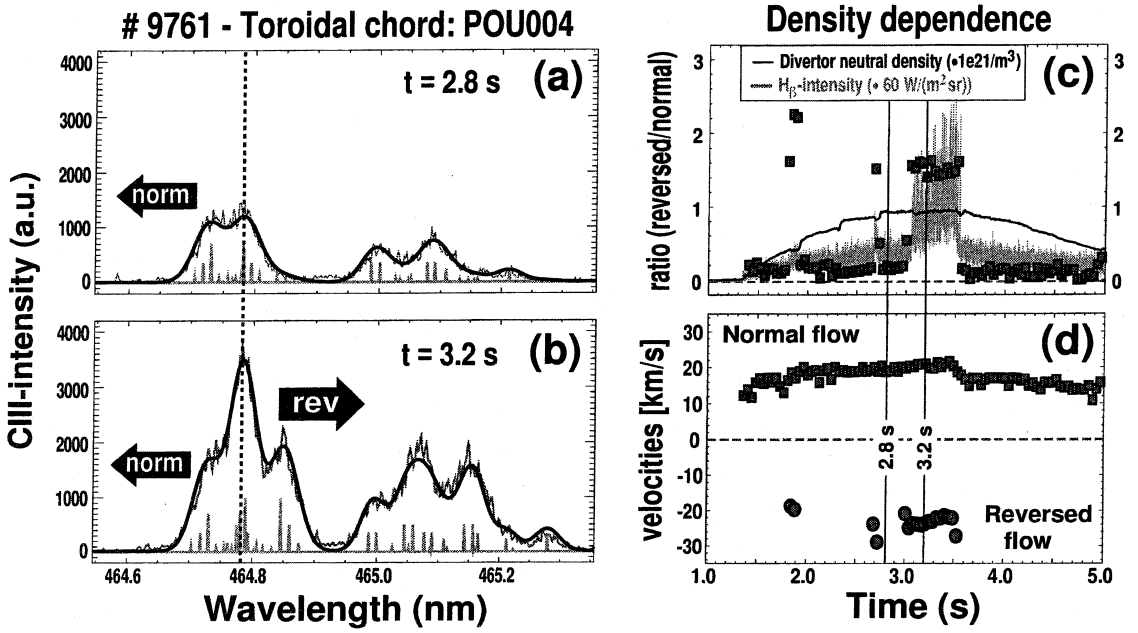

Fig. 4. Spectroscopic observation of C^{2+}-flow reversal in toroidal chord POU004 (near separatrix; cf. Fig. 1(b)) in an L-mode density ramp: (a) blue-shifted CIII-spectrum ($t = 2.8$ s; attached); (b) superposition of additional red-shifted CIII-component (reversed flow) onto blue-shifted one ($t = 3.2$ s; detached); (c) ratio (reversed/normal), divertor neutral density and H_β-emission (outer separatrix) as detachment monitor; (d) resulting C^{2+}-flow velocities.

indicating zero-shift), the latter one (Fig. 4(b)) obviously shows a significantly changed line-shape that is brought about by the additional red-shifted component which is created by flow reversal of C^{2+}-ions. The numerical fit yields a larger magnetic field (Zeeman splitting $\rightarrow \approx 2.7$ T) for the reversed component which is in accordance with the expectation that the – spectroscopically detectable – flow reversal zones are located at somewhat smaller radii ($R \approx 1.54$ and 1.65 m) than the region of 'usual' flow ($R \approx 1.68$ m) directed towards the plates ($\rightarrow \approx 2.5$ T; comp. Fig. 3).

Fig. 4(c) and (d) summarize the results on C^{2+}-flows for this discharge (# 9761): Fig. 4(c) contains the time evolution of divertor neutral density and the resulting H_β-intensity (at the separatrix) which is to be used as a detachment indicator according to the discussion in Section 2: detachment enhances volume recombination, and thereby, the emission of neutral hydrogen. The squares represent the intensity ratio of the reversed to the normal CIII-component obtained from the numerical fit to the spectra. This ratio is used to discriminate the reversed flow velocities that are reliable by setting a detection threshold (0.25 in this case). It may be possible to increase the detection sensitivity by using a theoretical lineshape accounting precisely for atomic sublevel splitting caused by the Zeeman–/Paschen–Back effect [6]. However, for the pronounced variations of the CIII-spectra discussed here, it is fully sufficient to use a less voluminous fit function based on Zeeman effect and $\cdot\cdot$-coupling [2].

In Fig. 4(d) the resulting velocities are plotted: while the normal flow can be seen during the whole discharge, the reversed flow is only detectable unambiguously if the intensity ratio (squares in Fig. 4(c)) of red- to blue-shifted component is greater than about 0.25. This is obviously only the case if the plasma is detached enough (see H_β in Fig. 4(c)) to provide the required CIII-emission in the flow reversal zone located more upstream. As soon as the plasma attaches again the reversed CIII-component vanishes. However, this does not necessarily mean that the flow reversal itself disappears, because the emission zone just might shift out of the flow reversal zone. The data show that the reversed flow velocity lies between 20 and 30 km/s and is in good agreement with the respective 2D-code results: for this L-mode density ramp a detailed B2-EIRENE simulation was especially performed for the experimental conditions. In order to compare experiment and modeling we selected a run with parameters matched to the actual discharge with respect to the power into the SOL (4 MW), SOL-density (2.5×10^{19} m^{-3}), carbon and hydrogen radiation and the respective distributions in the divertor. For the same conditions in which we observed flow reversal of C^{2+}, B2-EIRENE yields a (chord averaged) 'forward' velocity of about 20 km/s and a reversed velocity of 15–20 km/s. The measured values (Fig. 4(d)) are about 21 and 22–25 km/s, respectively. Hence, B2-EIRENE predictions have not only been validated qualitatively by the spectroscopic observation of impurity flow reversal, but there is also a good quantitative agreement.

Further support for modeling comes from recent ASDEX Upgrade discharges in which the line averaged electron density was ramped up to 1.1×10^{20} m^{-3}. This upper value corresponds to a SOL-density of 3.6×10^{19} m^{-3} measured in the midplane. The respective spectroscopic data confirm the expectation discussed above that flow reversal should only be detectable in a limited density range where the thermal forces as well as the required overlap of emission and flow reversal zones are sufficient: flow reversal of C^{2+} first appeared and then disappeared again before the density had reached its maximum value. However, it must be borne in mind that the disappearance of the flow reversed component from the CIII-spectrum may only be caused by a lack of detectability which is mainly due to the insufficient overlap discussed above. Accordingly, this does not necessarily mean that flow reversal itself has stopped.

4. Discussion

Coming back to the question of main plasma contamination that might be caused by impurity flow reversal, we note that no significant increase of Z_{eff} in the core was observed in the respective time range of about 0.5 s. A reason for this, suggested by B2-EIRENE modeling results, might be that due to the existence of radial transport one gets the formation of large-scale convective cells, and consequently, an effective global mixing in the whole divertor. In regions where flow reversal appears the Mach number of the fuel ions is expected to be rather low (below 0.05). Accordingly, the radial transport brings the impurities during the backflow into regions where they experience again forces directed towards the target plates. Therefore, it seems that flow reversal mainly leads to a redistribution of impurities in the divertor with the retention capability not being affected severely even at the high densities needed for (partial) detachment.

References

[1] J. Neuhauser et al., J. Nucl. Mater. 121 (1984) 194.
[2] J. Gafert et al., Plasma Phys. Control. Fusion 39 (1997) 1981.
[3] D. Reiter, J. Nucl. Mater. 196–198 (1992) 80.
[4] J. Gafert et al., Europhys. Conf. Abstr. Part IV, 21A (1997) 1397.
[5] R. Schneider et al., these Proceedings.
[6] R.C. Isler, Phys. Plasmas 4 (1997) 355.